Nonlinear Model-Based Control of an Experimental Reverse Osmosis Water Desalination System ⋆

Alex R. Bartman, [*] **Panagiotis D. Christofides,** [*,**,1] **Yoram Cohen** [*]

[*] *Department of Chemical and Biomolecular Engineering, University of California, Los Angeles, CA 90095-1592 USA.*
[**] *Department of Electrical Engineering, University of California, Los Angeles, CA 90095-1592, USA.*

Abstract: This work focuses on the design and implementation of a nonlinear model-based control system on an experimental reverse osmosis (RO) membrane water desalination system in order to deal with large set-point changes and variations in feed water salinity. A dynamic nonlinear lumped-parameter model is derived using first-principles and its parameters are computed from experimental data to minimize the error between model predictions and experimental RO system response. Then, this model is used as the basis for the design of a nonlinear control system using geometric control techniques. The nonlinear control system is implemented on the experimental RO system and its set-point tracking capabilities are successfully evaluated.

Keywords: Process control, process monitoring, model based control, nonlinear process systems

1. INTRODUCTION

Reverse osmosis (RO) membrane desalination has emerged as one of the leading methods for water desalination due to the low cost and energy efficiency of the process (Rahardianto et al. (2007)). Lack of fresh water sources has necessitated further development of these desalination plants, especially in areas with dry climates. Even with advances in reverse osmosis membrane technology, maintaining the desired process conditions is essential to successfully operating a reverse osmosis desalination system. Seasonal, monthly, or even daily changes in feed water quality can drastically alter the conditions in the reverse osmosis membrane modules, leading to decreased water production, sub-optimal system performance, or even permanent membrane damage. In order to account for the variability of feed water quality, a robust process control strategy is necessary. In a modern reverse osmosis (RO) plant, automation and reliability are elements crucial to personnel safety, product water quality, meeting environmental constraints, and satisfying economic demands. Industrial reverse osmosis desalination processes primarily use traditional proportional and proportional-integral control to monitor production flow and adjust feed pumps accordingly (Alatiqi et al. (1999)). While such control strategies are able to maintain a consistent product water (permeate) flow rate, they may fail to provide an optimal closed-loop response with respect to set-point transitions owing to the presence of nonlinear process behavior (Chen et al. (2005)). In some cases, permeate production can decrease due to scaling or fouling on the membrane surface. When this occurs, traditional control algorithms force the feed pumps to increase feed flow rate leading to an increased rate of scaling, irreversible membrane damage, and eventual plant shutdown. Traditional process control schemes are also unable to monitor plant energy usage and make adjustments toward energy-optimal operation. Model based control is a promising alternative to traditional RO plant control strategies. Several model based methods such as model-predictive control (MPC) and Lyapunov-based control have been evaluated via computer simulations for use in reverse osmosis desalination (Abbas (2006); McFall et al. (2008); Bartman et al. (2009b); Gambier and Badreddin (2002)). Experimental system identification and MPC applications can also be found in the literature (Assef et al. (1997); Burden et al. (2001)). Model based control methods have also been used in conjunction with fault detection and isolation schemes to improve robustness of control methods in the presence of sensor and actuator failures (McFall et al. (2008)). Other automatic control methods utilize model based control based on a linear model (Alatiqi et al. (1989)); using step tests to create a model that is a linear approximation around the desired operating point. Several other traditional control methods have also been studied in the context of RO system integration with renewable energy sources (Herold and Neskakis (2001); Liu et al. (2002)). Motivated by these considerations, the goal of this work is to evaluate the effectiveness of a feedback linearizing nonlinear model-based controller through application to an experimental reverse osmosis desalination system. The nonlinear model-based controller is shown to possess excellent set-point tracking capabilities. The nonlinear controller is also shown to outperform a proportional-integral control system.

⋆ Financial support from NSF and the California Department of Water Resources is gratefully acknowledged.
[1] Corresponding author: P.D. Christofides, pdc@seas.ucla.edu

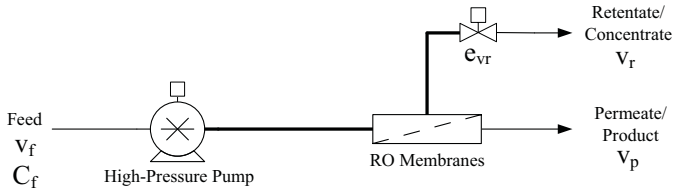

Fig. 1. Reverse osmosis system used for model development

2. RO SYSTEM MODEL

In this section, a fundamental model of a representative RO desalination system is developed including all of the basic elements present in UCLA's experimental RO desalination system. In this system, shown in Fig. 1, water enters the feed pump, which is equipped with a variable frequency drive (VFD), and is pressurized to the feed pressure P_{sys}. The pressurized stream enters the membrane module where it is separated into a low-salinity product (or permeate) stream with velocity v_p, and a high-salinity brine (or retentate) stream with velocity v_r. In the model, the individual spiral-wound membranes in series are assumed to be one large spiral-wound membrane in one large vessel, where any effects of individual membrane vessel interconnections are neglected. The pressure downstream of the actuated valve and at the permeate outlet is assumed to be equal to atmospheric pressure.

The model is based on a mass balance taken around the entire system and an energy balance taken around the actuated retentate valve. In the model derivation, it is assumed that the water is an incompressible fluid, all components are operated on the same plane (so potential energy terms due to gravity can be neglected), and the density of the water is assumed to be constant. It is also assumed that the effective concentration in the membrane module is a weighted average of the feed concentration and the brine stream concentration (see Eq. 6 below). The model derivation results in a nonlinear ordinary differential equation for the retentate stream velocity and an algebraic relation for the system pressure. This model is an adaptation of a model developed in our previous work used to describe a similar reverse osmosis desalination system (McFall et al. (2008)). In the previous work, the system utilized a feed pump with a constant feed flow rate, but used a separate bypass stream with an actuated valve to control the velocity of the water feeding to the membrane units. An equation for the osmotic pressure based on effective concentration and temperature in the membrane unit was also developed in (Lu et al. (2007)), and is used as an estimate in the model. Specifically, an energy balance is first taken around the retentate valve which leads to the following differential equation:

$$\frac{dv_r}{dt} = \frac{P_{sys}A_p}{\rho V} - \frac{1}{2}\frac{A_p e_{vr} v_r^2}{V} \tag{1}$$

where v_r is the retentate stream velocity, P_{sys} is the system pressure, A_p is the pipe cross-sectional area, ρ is the fluid density, V is the system volume and e_{vr} is the retentate valve resistance. To compute an expression for the system pressure in terms of the other process variables, an overall steady-state mass balance is taken to yield:

$$0 = v_f - v_r - v_p \tag{2}$$

where v_f is the feed stream velocity and v_p is the permeate stream velocity. In order to get an expression for the system pressure, the following classical expression is used for the computation of the permeate stream velocity:

$$v_p = \frac{A_m K_m}{\rho A_p}(P_{sys} - \Delta\pi) \tag{3}$$

where A_m is the membrane area, K_m is the membrane overall mass transfer coefficient, and $\Delta\pi$ is the difference in osmotic pressure between the feed side of the membrane and the permeate side. Substituting Eq. 3 into Eq. 2, the following expression for the system pressure (P_{sys}) is obtained:

$$P_{sys} = \frac{\rho A_p}{A_m K_m}(v_f - v_r) + \Delta\pi \tag{4}$$

where the osmotic pressure ($\Delta\pi$) and effective average concentration at the membrane surface (C_{eff}) on the feed side can be computed from the following relations:

$$\Delta\pi = \delta C_{eff}(T + 273) \tag{5}$$

$$C_{eff} = C_f(a + (1-a)((1-R) + R(\frac{v_f}{v_r}))) \tag{6}$$

where C_f is the amount of total dissolved solids (TDS) in the feed, a is an effective concentration weighting coefficient, δ is a constant relating effective concentration to osmotic pressure, T is the water temperature in degrees Celsius, and R is the fractional salt rejection of the membrane. Substituting Eq. 4 into the energy balance equation of Eq. 1 yields the following nonlinear ordinary differential equation for the dynamics of the retentate stream velocity:

$$\frac{dv_r}{dt} = \frac{A_p^2}{A_m K_m V}(v_f - v_r) + \frac{A_p}{\rho V}\Delta\pi - \frac{1}{2}\frac{A_p e_{vr} v_r^2}{V} \tag{7}$$

Using the above dynamic equation, various control techniques can be applied using the valve resistance value (e_{vr}) as the manipulated input. As the valve resistance goes to zero, the valve behaves as an open pipe; as the valve resistance approaches infinity, the valve behaves as a total obstruction and the flow velocity goes to zero (Bird et al. (2002)). To accurately model the valve dynamics and to relate the experimental results to the concept of valve resistance value (e_{vr}), the concept of valve C_v is used. The definition of C_v for a valve in a water system is:

$$C_v = \frac{Q_r}{\sqrt{P_{sys}}} \tag{8}$$

where Q_r is the volumetric flow rate ($Q_r = A_p v_r$) through the retentate valve. In order to obtain an expression for C_v as a function of the retentate valve resistance (e_{vr}), we consider the steady state form of the energy balance of Eq. 1, solve the resulting equation for P_{sys} and substitute the resulting expression for P_{sys} into Eq. 8 to yield:

$$C_v = \frac{A_p}{\sqrt{\frac{1}{2}\rho e_{vr}}} \tag{9}$$

Depending on the type of valve and its flow characteristics, it is assumed that the C_v values (and in turn, the e_{vr}

values) can be related to the valve position (percentage open) through the following empirical logarithmic relation based on commercially available valve data (Bartman et al. (2009b)):

$$O_p = \mu \ln e_{vr} + \phi \tag{10}$$

where μ and ϕ are constants depending on the valve properties. The values of μ and ϕ for this model are taken from a paper based on the same experimental system at UCLA (Bartman et al. (2009b)). For the model presented in this paper, the curve relating valve position (O_p) to resistance value (e_{vr}) is shown in Fig. 2. It can be seen in Fig. 2 that as the valve position goes to zero (fully closed), the valve resistance values begin to grow at an increasing rate; and as the valve approaches the fully-open position, the resistance values change slowly. The data from the experimental system is also plotted on the figure, and it can be seen that the data does not fit the same logarithmic relation as the ideal valve curve. Due to the shape of the experimental data curve, the data is fit in three segments with curve fits following a similar form as the theoretical curve. The first curve fit is applied to valve resistance (e_{vr}) values of approximately 205 to 212 and takes the form:

$$O_p = -84.428 \ln(e_{vr}) + 459.21 \tag{11}$$

For e_{vr} values between 212 and 6200, O_p is computed by:

$$O_p = -2.0473 \ln(e_{vr}) + 18.141 \tag{12}$$

while for e_{vr} values above 6200, O_p is computed by:

$$O_p = -0.0778 \ln(e_{vr}) + 0.9476 \tag{13}$$

This treatment of the valve characteristics allows for conversion of the experimental values of O_p to values of e_{vr} in the model-based nonlinear control algorithm, and allows for values of e_{vr} generated by the control algorithm to be translated to values of O_p to be sent to the actuated valve on the experimental system. Capturing the nonlinearity present in the valve is extremely crucial when applying the control algorithms to the experimental system.

2.1 Computation of Nonlinear Model Parameters Based on Experimental Data

Most of the parameters of the model of Eqs. 7-13 such as the membrane area (A_m), water density (ρ), pipe cross-sectional area (A_p), and system volume (V) have constant values which can be obtained from the experimental system. Another key model parameter, the overall mass transfer coefficient (K_m) was computed to match the model response to experimental step-test data. Specifically, K_m was computed using steady state data from the experimental system by minimizing the difference between the model steady state and the experimental system steady state for various step tests. The computed values of K_m were then averaged to determine the best value for use in the model used for controller design. The values of the model parameters can be found in Table 1.

3. CONTROL ALGORITHMS

Two separate control loops are present in the control problem formulation. The first loop regulates the system pressure by adjusting the variable frequency drive (VFD) speed directly (effectively changing the feed flow rate). This control loop will be termed "loop I". In each set of experiments presented below, a proportional-integral (PI) feedback controller is used to keep the system pressure (P_{sys}) at the set-point value (P_{sys}^{sp}) of 150 psi. This control algorithm takes the form:

$$S_{VFD} = K_f(P_{sys}^{sp} - P_{sys}) + \frac{K_f}{\tau_f}\int_0^{t_c}(P_{sys}^{sp} - P_{sys})dt \tag{14}$$

where S_{VFD} is the control action applied to the variable frequency drives (VFD speed), K_f is the proportional gain and τ_f is the integral time constant. The second control loop (termed "loop II") uses a nonlinear model-based controller (for the purposes of comparison, and a PI controller is also used in loop II). The nonlinear controller utilizes the error between the retentate velocity and its corresponding set-point, but it also takes into account many additional system variables (El-Farra and Christofides (2001, 2003); Christofides and El-Farra (2005)). Specifically, the nonlinear model-based controller manipulates the actuated retentate valve position by using measurements of the feed flow velocity (v_f), feed salinity (C_f), and retentate flow velocity (v_r). The nonlinear controller is designed following a feedback linearization approach. To derive the controller formula, the following linear, first-order response in the closed-loop system between v_r and v_r^{sp} is requested:

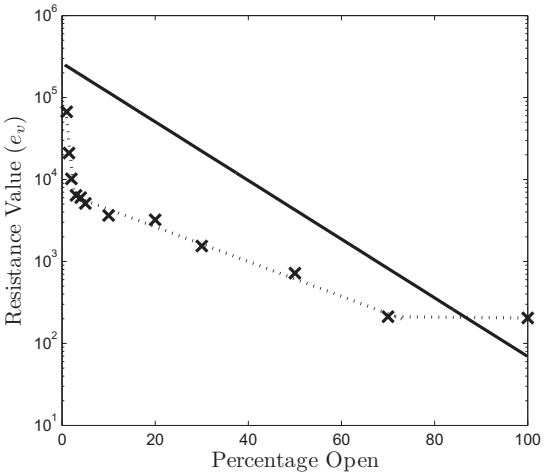

Fig. 2. Correlation between valve resistance value (e_{vr}) and valve percentage open (O_p) : commercial theoretical data (solid line), experimentally measured data (x), and curve fittings to experimental data (dashed lines) using Eqs. 11-13.

Table 1. Process model parameters based on experimental system data.

ρ	=	1007	kg/m^3
V	=	0.6	m^3
A_p	=	0.000127	m^2
A_m	=	15.6	m^2
K_m	=	6.4×10^{-9}	s/m
C_f	=	4842	mg/L
a	=	0.5	
T	=	22	$^\circ C$
R	=	0.97	

$$\frac{dv_r}{dt} = \frac{1}{\gamma}(v_r^{sp} - v_r) \tag{15}$$

It is noted that a first-order response is requested because the relative degree between v_r and e_{vr} is one (Christofides and El-Farra (2005)). Using this approach, the following formula is obtained for the nonlinear controller:

$$e_{vr} = \frac{\frac{1}{\gamma}(v_r^{sp} - v_r) - \frac{A_p^2}{A_m K_m V}(v_f - v_r) - \frac{A_p \delta (T+273)}{\rho V} C_{eff}}{\frac{-A_p}{2V}(v_r^2)} \tag{16}$$

To achieve offset-less response, integral action is added to the controller in Eq. 16 and the resulting controller takes the form:

$$e_{vr} = \frac{\frac{1}{\gamma}(v_r^{sp} - v_r) + \frac{1}{\tau_{NL}}\int_0^{t_c}(v_r^{sp} - v_r)dt}{\frac{-A_p}{2V}(v_r^2)} + \frac{-\frac{A_p^2}{A_m K_m V}(v_f - v_r) - \frac{A_p \delta (T+273)}{\rho V} C_{eff}}{\frac{-A_p}{2V}(v_r^2)} \tag{17}$$

As a baseline, the performance of the nonlinear controller is compared to a traditional form of control. Loop II, using PI control, uses the retentate (or concentrate) stream flow velocity to manipulate the actuated valve in order to regulate the retentate stream velocity/flow rate. Under PI control, the control system for loop II takes the form:

$$O_p = K_r(Q_r^{sp} - Q_r) + \frac{K_r}{\tau_r}\int_0^{t_c}(Q_r^{sp} - Q_r)dt \tag{18}$$

where Q_r is the retentate stream volumetric flow rate and Q_r^{sp} is the retentate stream flow rate set-point. In the experiments, the performance of the nonlinear controller implemented on the experimental system is compared to the performance of the nonlinear controller implemented on the process model and to the performance of the proportional-integral controller implemented on the experimental system. The control algorithms were programmed into the data acquisition and control software to operate in real-time with a sampling time of 0.1 seconds. Additionally, the actuated retentate valve is powered by an electric motor with a maximum operating speed which must be taken into account when attempting to simulate the nonlinear controller action. From testing on the experimental system, it was found that the actuated valve could travel its entire range in approximately 45 seconds; this provides an important constraint on the speed of valve opening/closing in the simulations of the form:

$$\left|\frac{dO_p}{dt}\right| \leq 2.22\frac{\%}{s} \tag{19}$$

To derive the constraint of Eq. 19, it is assumed that the valve speed is independent of valve position (valve always turns at maximum speed). This is a physical constraint which is intrinsically accounted for in the experimental results and is programmed into the nonlinear model-based controller simulation as well (to facilitate comparison). Additionally, when using the experimental system, the valve position is not allowed to fall under 1%, and any values sent to the valve above 100% are translated to the max value of 100% open. The lower constraint ($< 1\%$) is enforced so that the system pressure will not rise too rapidly. A constraint on the variable frequency drive is also placed to avoid pressure spikes (a maximum VFD speed of 4.5/10 is used). In the experiments presented in this work, the actuators do not reach these constraints.

4. EXPERIMENTAL SYSTEM DESCRIPTION

The experimental reverse osmosis water desalination system constructed at UCLA's Water Technology Research (WaTeR) Center was used for conducting the control experiments. This experimental system is comprised of a feed tank, two low-pressure feed pumps in parallel which provide enough pressure to pass the feed water through a series of cartridge filters while also providing sufficient pressure for operation of the high-pressure pumps, two high-pressure pumps in parallel (each capable of delivering approximately 4.3 gallons per minute at 1000 psi), and a bank of 18 pressure vessels containing Filmtec spiral-wound RO membranes. The high-pressure pumps are outfitted with variable frequency (or variable speed) drives which enable the control system to adjust the feed flow rate by using a 0-10V output signal. The bank of 18 membranes are arranged into 3 sets of 6 membranes in series; and for the control experiments presented below, only one bank of 6 membrane units was used. The experimental system uses solenoid valves controlled by the data acquisition and control hardware to enable switching between multiple arrangements of the membrane modules (2 banks of 6 in parallel to one bank of 6 in series, or any number of the modules in series) while also allowing for control of the flow direction through the membrane banks. After the membrane banks, an actuated valve is present to control the cross-flow velocity (v_r) in the membrane units, while also influencing system pressure. This valve is used as an actuator for the control system utilizing the control algorithms presented in section 3. The resulting permeate and retentate streams are currently fed back to the tank in an overall recycle mode, but for field operation the system can be operated in a one-pass fashion. The experimental system also has an extensive sensor and data acquisition network; flow rates and stream conductivities are available in real-time for the feed stream, retentate stream and permeate stream. The pressures before each high pressure pump, as well as the pressures before and after the membrane units (feed pressure and retentate pressure) are also measured. The system also includes sensors for measuring feed pH, permeate pH, in-tank turbidity, and feed turbidity after filtration (in real-time). A centralized data acquisition system takes all of the sensor outputs (0-5V, 0-10V, 4-20mA) and converts them to process variable values on the local (and web-accessible) user interface where the control system is implemented. The data is logged on a local computer as well as on a network database where the data can be accessed via the internet, while the control portion of the web-based user interface is only available to persons with proper authorization. The data acquisition and control system uses National Instruments software and hardware to collect the data at a sampling rate of 10 Hz and perform the necessary control calculations needed for the computation of the control action to be implemented by the control actuators. A photograph of the system can be seen in Fig. 3.

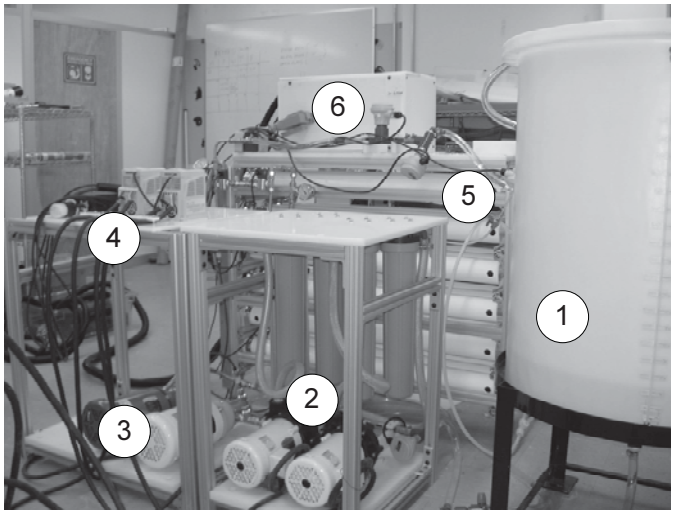

Fig. 3. UCLA experimental RO membrane water desalination system: (1) Feed tank, (2) Low-pressure pumps and prefiltration, (3) High-pressure positive displacement pumps, (4) Variable frequency drives (VFDs), (5) Pressure vessels containing spiral-wound membrane units (3 sets of 6 membranes in series), (6) National Instruments data acquisition hardware and various sensors.

5. EXPERIMENTAL CLOSED-LOOP RESULTS

In the control experiments presented in this paper, the experimental system was turned on and the PI loop controlling the variable frequency drives (loop I) was activated to bring the system pressure to a set-point of $P_{sys} = 150$ psi. The retentate flow rate was set to 1.5 gallons per minute (gpm). After the system had been operating at this steady state for a sufficient period of time, loop II was activated to manipulate the retentate valve. All data taken from the experimental system was averaged (after the experiments) using a 19 point moving average to remove most of the measurement noise. The following sets of experiments compare the performance of the nonlinear controller with the performance of the proportional and proportional-integral controllers. The closed-loop response observed for the nonlinear controller applied to the dynamic process model is used as a baseline for comparison of controller performance, as well as to determine an approximate range of controller tunings for the experimental system. In this set of experiments, the retentate flow rate set-point was changed from an initial value of 1.5 gpm to a new value of 0.8 gpm, while the VFD control loop is again maintained at a pressure set-point of 150 psi. In this set of experiments, the performance of the nonlinear controller with integral term is evaluated against the performance of a proportional-integral (PI) controller (both of these controllers are implemented experimentally), and the performance of the nonlinear controller with integral action applied to the dynamic process model via simulations. The feed salt concentration for these experiments was approximately 8200 ppm of NaCl. The tuning parameters for the controllers in this set of experiments can be found in Tables 2 and 3.

The results for these experiments are plotted in Figs. 4 - 5. In Fig. 4, it can be seen that all of the closed-loop results (simulated and experimental) decrease at the same rate initially (due to the valve opening/closing rate constraint). As expected, the simulated nonlinear model-based controller with integral term immediately converges to the set-point with no offset since it is not subject to any plant-model mismatch or measurement noise. As it is evident in Table 2, the integral time constant for the simulated controller is slightly different ($\tau_f = 0.01$, $\tau_f^{sim} = 0.0091$). The simulations where the nonlinear controller was applied to the process model were used to find an approximate range of controller parameters, but these values were implemented on the experimental system and changed slightly to achieve better closed-loop performance in the presence of plant-model mismatch. The speed of the closed-loop response under the nonlinear controller applied to the experimental system is slower in terms of convergence to the set-point than the one in the simulated case and the retentate flow rate reaches the set-point in about 145 seconds. The proportional-integral

Table 2. Loop I PI controller tuning parameters.

K_f	=	0.01
τ_f	=	0.1
K_f^{sim}	=	0.0091
τ_f^{sim}	=	0.1

Table 3. Loop II controller tuning parameters (both PI and nonlinear controllers).

K_r	=	1
τ_r	=	5
γ	=	0.6
τ_{NL}	=	10
γ^{sim}	=	0.6
τ_{NL}^{sim}	=	10

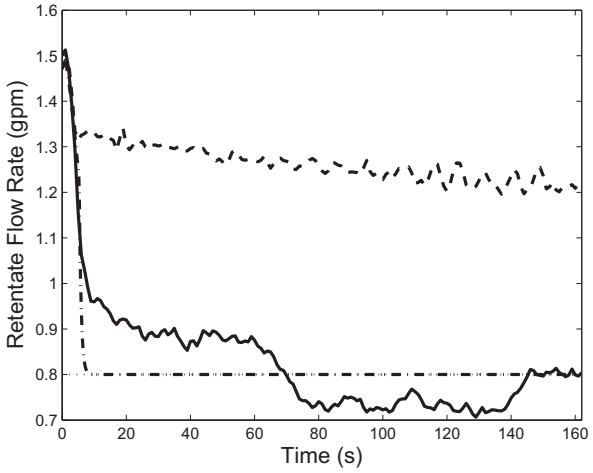

Fig. 4. Profiles of retentate flow rate (Q_r) with respect to time for retentate flow rate set-point transition from 1.5 to 0.8 gpm under proportional-integral control (dashed line), nonlinear model-based control with integral action (solid line) and nonlinear model-based control with integral action implemented via simulation on the process model (dash-dotted line). The horizontal dotted line denotes the retentate flow rate set-point ($Q_r^{sp} = 0.8$ gpm).

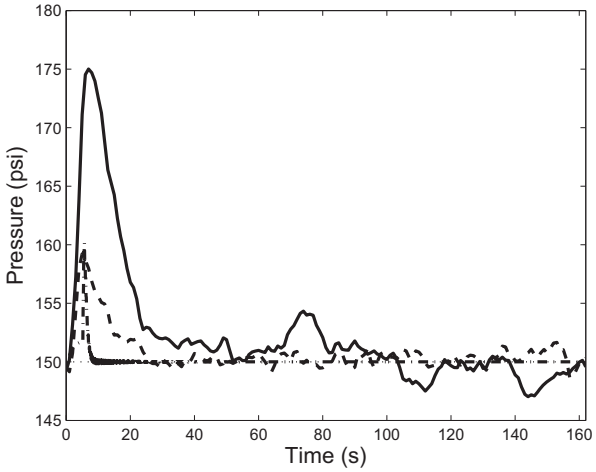

Fig. 5. Profiles of system pressure (P_{sys}) with respect to time for retentate flow rate set-point transition from 1.5 to 0.8 gpm under proportional-integral control (dashed line), nonlinear model-based control with integral action (solid line) and nonlinear model-based control with integral action implemented via simulation on the process model (dash-dotted line). The horizontal dotted line denotes the system pressure set-point ($P_{sys}^{sp} = 150$ psi).

(PI) controller with $\tau_r = 5$ leads to an extremely slow convergence to the set-point (on the order of 10 minutes). It is also seen that when a smaller integral time constant is used, it results in significant oscillations around the set-point due to the coupling between the two control loops. These oscillations cause large fluctuations in the feed flow rate (due to the VFD control loop) and could damage the feed pumps and cause fatigue on system components. Similar results are evident in Fig. 5. The application of the nonlinear controller to the experimental system causes the most deviation from the pressure set-point due to the speed at which it converges to the set-point. It can be seen that the PI controller causes almost no deviation from the set-point (approximately the same as the simulated nonlinear controller) because the convergence (change in valve position) is much slower. As the valve closes, it causes the system pressure to rise, forcing loop I to take action in order to keep the system pressure at the set-point. Slower valve actions allow more time for loop I to act and keep the system pressure at the set-point, such as in the case of the PI control with $\tau_r = 5$. Additional results from the experiments can be seen in the submitted journal paper (Bartman et al. (2009a)).

REFERENCES

Abbas, A. (2006). Model predictive control of a reverse osmosis desalination unit. *Desalination*, 194, 268–280.

Alatiqi, I., Ettourney, H., and El-Dessouky, H. (1999). Process control in water desalination industry: an overview. *Desalination*, 126, 15–32.

Alatiqi, I.M., Ghabris, A.H., and Ebrahim, S. (1989). System identification and control of reverse osmosis desalination. *Desalination*, 75, 119–140.

Assef, J.Z., Watters, J.C., Deshpande, P.B., and Alatiqi, I.M. (1997). Advanced control of a reverse osmosis desalination unit. *J. Proc. Cont.*, 4, 283–289.

Bartman, A.R., Christofides, P.D., and Cohen, Y. (2009a). Nonlinear model-based control of an experimental reverse osmosis water desalination system. *Industrial & Engineering Chemistry Research,* submitted.

Bartman, A.R., McFall, C.W., Christofides, P.D., and Cohen, Y. (2009b). Model predictive control of feed flow reversal in a reverse osmosis desalination process. *J. Process Contr.*, 19, 433–442.

Bird, R.B., Stewart, W.E., and Lightfoot, E.N. (2002). *Transport Phenomena, Second Edition.* John Wiley and Sons.

Burden, A.C., Deshpande, P.B., and Watters, J.C. (2001). Advanced control of a B-9 Permasep permeator desalination pilot plant. *Desalination*, 133, 271–283.

Chen, J., Wang, F., Meybeck, M., He, D., Xia, X., and Zhang, L. (2005). Spatial and temporal analysis of water chemistry records (19582000) in the Huanghe (Yellow River) basin. *Global Biogeochem. Cycles*, 19, GB3016.

Christofides, P.D. and El-Farra, N.H. (2005). *Control of Nonlinear and Hybrid Process Systems: Designs for Uncertainty, Constraints and Time-Delays,* 446 pages. Springer, New York.

El-Farra, N.H. and Christofides, P.D. (2001). Integrating robustness, optimality, and constraints in control of nonlinear processes. *Chemical Engineering Science*, 56, 1841–1868.

El-Farra, N.H. and Christofides, P.D. (2003). Bounded robust control of constrained multivariable nonlinear processes. *Chemical Engineering Science*, 58, 3025–3047.

Gambier, A. and Badreddin, E. (2002). Application of hybrid modeling and control techniques to desalination plants. *Desalination*, 152, 175–184.

Herold, D. and Neskakis, A. (2001). A small PV-driven reverse osmosis desalination plant on the island of gran canaria. *Desalination*, 137, 285–292.

Liu, C.C.K., Park, J., Migita, R., and Qin, G. (2002). Experiments of a prototype wind-driven reverse osmosis desalination system with feedback control. *Desalination*, 150, 277–287.

Lu, Y., Hu, Y., Zhang, X., Wu, L., and Liu, Q. (2007). Optimum design of reverse osmosis system under different feed concentration and product specification. *Journal of Membrane Science*, 287, 219–229.

McFall, C.W., Bartman, A.R., Christofides, P.D., and Cohen, Y. (2008). Control and monitoring of a high-recovery reverse-osmosis desalination process. *Industrial & Engineering Chemistry Research*, 47, 6698–6710.

Rahardianto, A., Gao, J., Gabelich, C.J., Williams, M.D., and Cohen, Y. (2007). High recovery membrane desalting of low-salinity brackish water: Integration of accelerated precipitation softening with membrane RO. *Journal of Membrane Science*, 289, 123–137.